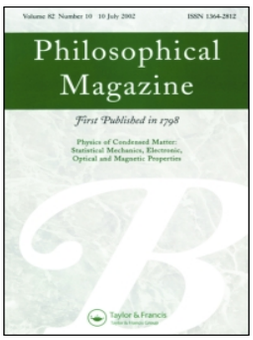

Philosophical Magazine B

ISSN: 1364-2812 (Print) 1463-6417 (Online) Journal homepage: https://www.tandfonline.com/loi/tphb20

Calculation of the electron-beam-induced current (EBIC) at a Schottky contact and comparison with Au/n-Ge diodes

Nouar Tabet & René Jean Tarento

To cite this article: Nouar Tabet & René Jean Tarento (1989) Calculation of the electron-beam-induced current (EBIC) at a Schottky contact and comparison with Au/n-Ge diodes, Philosophical Magazine B, 59:2, 243-261, DOI: 10.1080/13642818908220175

To link to this article: https://doi.org/10.1080/13642818908220175

Published online: 20 Aug 2006.

PHILOSOPHICAL MAGAZINE B, 1989, VOL. 59, NO. 2, 243–261

Calculation of the electron-beam-induced current (EBIC) at a Schottky contact and comparison with Au/n-Ge diodes

By NOUAR TABET† and RENÉ-JEAN TARENTO

Laboratoire de Physique des Matériaux, C.N.R.S., 92195 Meudon, France

[*Received 1 December 1987‡ and accepted 26 May 1988*]

ABSTRACT

The electron-beam-induced current (EBIC) collection efficiency η of a Schottky contact perpendicular to the electron beam of a scanning electron microscope is calculated. The continuity equation is solved for a non-uniform generation function assuming a linear variation of the electric field within the depletion zone. The recombination of the carriers at the metal–semiconductor interface is considered. Majority carrier injection from the semiconductor into the metal is found to be non-negligible for low doping level and low beam energy. It is demonstrated that the assumption of 100% collection efficiency for the minority carriers generated within the depletion zone, and the related boundary condition, lead to an overestimation of the collected EBIC intensity, particularly for short minority diffusion lengths. The present model allows a more satisfactory analysis of the experimental data obtained on Au/n-Ge Schottky contacts.

§ 1. INTRODUCTION

The electron-beam-induced current (EBIC) technique has been extensively used to characterize the electrical properties of semiconductors (Leamy 1982, Holt, Muir, Grant and Boswarva 1974, Sieber 1987). Besides defect imaging, the technique allows the determination of some parameters which describe the recombination process of the minority carriers, such as the diffusion length L_p, the lifetime τ_p and the recombination velocity S_p at surfaces or interfaces. Wu and Wittry (1978) proposed a method to deduce L_p from collection efficiency measurements on a Schottky contact parallel to the bombarded surface. They derived an analytical expression for the EBIC intensity and distinguished two main regions of the device: the metal where the incident beam loses a fraction of energy without producing any electron–hole pairs, the depletion zone (DZ) where all the generated minority carriers are collected with 100% efficiency, and the neutral zone where the carriers diffuse and are collected when they reach the limit of the DZ. The authors used the model successfully to fit their EBIC data obtained on Au–GaAs and Au–Si Schottky contacts. Less good agreement was pointed out by Wu and Wittry (1978) for lightly doped Si samples ($N_D = 10^{14}\,cm^{-3}$).

Otherwise it is well established that, for many materials, the formation of Schottky contacts can be related to the existence of interface states (Rhoderick 1978, Tersoff 1984). The recombination of carriers via such states has already been evoked to explain

† Permanent address: Laboratoire de Physique du Solide, Université de Constantine, Algeria.

‡ Received in final form 21 April 1988.

the low values of the collection efficiency of Au–InP Schottky contacts (Peransin, Da Silva and Bresse 1986), while in the Wu and Wittry model such recombination is not considered. Moreover the assumption of a 100% collection efficiency for the carriers which are generated within the DZ seems more valid near the interface, where the electric field intensity is a maximum, than at the limit of the neutral region where the electric field is null. Hence the boundary condition at the latter limit as it is written in the Wu and Wittry model, that is, the excess carrier Δp is null, seems rather artificial. In this paper, the continuity equation is solved assuming drift and diffusion of both minority and majority carriers in the DZ and using specific boundary conditions. The model is used to analyse experimental data obtained on Au–n-Ge contacts.

§2. Theory

2.1. *Preliminaries*

Figure 1 illustrates the device geometry. The metal layer of z_m thickness constitutes a region where a fraction of the incident beam energy is lost without producing any electron–hole pairs. In the absence of any defect, the collection probability of a carrier depends only on the depth z at which it is produced. Consequently, the collected EBIC intensity is independent of the lateral distribution of the pair generation function. Hence, for simplicity, we consider a one-dimensional problem. The continuity equation can be written in the following form:

$$dJ/dz = g(z) - r(z), \tag{1}$$

where J is the carrier flux, $g(z)$ and $r(z)$ are the generation and recombination rates ($cm^{-3}s^{-1}$) respectively. Following Wu and Wittry (1978), we use for the pair

Fig. 1

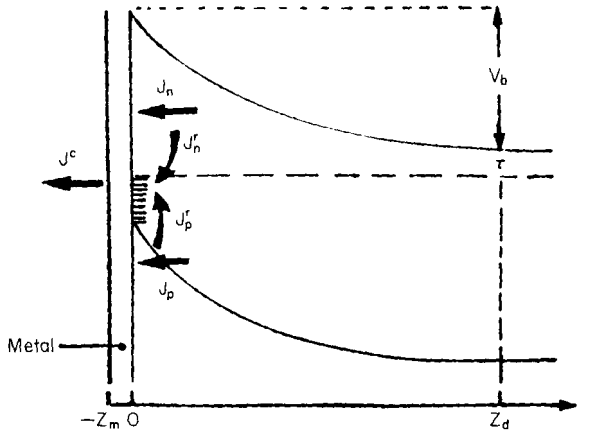

Schematic representation of the energy band diagram and the carrier fluxes at a metal/n-semiconductor Schottky contact.

generation function the modified Gaussian approximation to the depth distribution of the energy dissipation function $\phi(u)$ given by

$$\phi(u) = A \exp\left[-\left(\frac{u-u_0}{u}\right)^2\right] - B \exp\left(b\frac{u}{u_0}\right), \tag{2}$$

where $u = \rho z/R$, ρ is the density of the semiconductor in g cm^{-3}, z the depth (in cm) and R the electron penetration range (in g cm^{-2}).

R is given by Wittry and Kyser (1967) as

$$R\ (\text{g cm}^{-2}) = 2{\cdot}56 \times 10^{-3}\left(\frac{E_0}{30}\right)^{1{\cdot}7},$$

where E_0 is the beam energy (in keV).

The following values of the parameters in eqn. (2) were given by Wu and Wittry (1978) for GaAs as $u_0 = 0{\cdot}125$, $\Delta u = 0{\cdot}350$, $b = 4{\cdot}0$ and $B/A = 0{\cdot}4$. Since Ge and GaAs have the same atomic number ($Z = 32$), these values will be used below for computations of the collection efficiency of Au–Ge Schottky contacts.

The constants A and B can be determined using the normalization condition

$$\int_{-u_m}^{\infty} \phi(u + u_m)\, du = G_0 \tag{3}$$

(the coordinate origin is at the metal–semiconductor interface). Here $u_m = \rho_m z_m/R$, ρ_m being the metal density. G_0 is the total generation rate (in cm^2 s^{-1}) and can be expressed as

$$G_0 = \frac{J_0}{e}\frac{E_0}{\varepsilon_{e-h}}(1-f), \tag{4}$$

where J_0 and E_0 are the current and energy of the primary beam respectively, ε_{e-h} the electron–hole pair creation energy, f the fraction of the back-scattered energy, and e the charge on the electron. The generation rate $g(z)$ can be related to $\phi(u)$ by the following equation:

$$g(u) = (\rho/R)\phi(u + u_m). \tag{5}$$

2.2. *Carrier transport in the depletion zone*

We consider the case of an n-doped semiconductor. The continuity equation (eqn. (1)) can be written explicitly for the minority (holes) and majority (electrons) carriers, by first taking into account both diffusion and drift components of the fluxes:

$$J_p = -D_p(\Delta N_p/dz) + \Delta N_p \mu_p E(z), \tag{6}$$

$$J_n = -D_n(d\Delta N_n/dz) - \Delta N_n \mu_n E(z), \tag{7}$$

where D and μ are the diffusion coefficient and mobility of the carriers, ΔN_p and ΔN_n are the (positive) hole and electron excess densities respectively and E the electric field. $E(z)$ is obtained by solving the Gaussian equation

$$\frac{dE(z)}{dz} = \frac{N_d e}{\varepsilon}, \tag{8}$$

where N_d is the concentration of the ionized donors and ε the dielectric constant of the

semiconductor. Assuming a fully depleted zone, $E(z)$ is given by:

$$E(z)=(N_d e/\varepsilon)(z-z_d), \tag{9}$$

where z_d is the depletion depth.

Using eqns. (6) and (7), eqn. (1) can be written explicitly as

$$\left.\begin{aligned} -D_p\frac{d^2(\Delta N_p)}{dz^2}+\mu_p\frac{N_d e}{\varepsilon}(z-z_d)\frac{d(\Delta N_p)}{dz}+\mu_p\frac{N_d e}{\varepsilon}\Delta N_p=g(z)-r_p,\\ -D_n\frac{d^2(\Delta N_n)}{dz^2}-\mu_n\frac{N_d e}{\varepsilon}(z-z_d)\frac{d(\Delta N_n)}{dz}-\mu_n\frac{N_d e}{\varepsilon}\Delta N_n=g(z)-r_n. \end{aligned}\right\} \tag{10}$$

The recombination rates r_p and r_n can be related to the lifetimes τ_p and τ_n using the Hall–Schockley–Read theory:

$$r_p=\Delta N_p/\tau_p, \qquad r_n=\Delta N_n/\tau_n. \tag{11}$$

The values of τ_p and τ_n are z-dependent owing to the energy band curvature within the depletion zone. For simplicity, we consider in the present calculations that there is no recombination in the DZ, that is, $r_p=r_n=0$. Equations (10) can then be written in the form

$$\left.\begin{aligned} \frac{d^2(\Delta N_p)}{dz^2}+2\alpha(z-z_d)\frac{d(\Delta N_p)}{dz}+2\alpha\,\Delta N_p=\frac{g(z)}{D_p},\\ \frac{d^2(\Delta N_n)}{dz^2}-2\alpha(z-z_d)\frac{d(\Delta N_n)}{dz}-2\alpha\,\Delta N_n=\frac{g(z)}{D_n}, \end{aligned}\right\} \tag{12}$$

where $\alpha=N_D e^2/(2\varepsilon kT)$. (The Einstein equation $D/\mu=kT/e$ has been used to derive eqns. (12).)

The solutions of eqns. (12) are given by

$$\begin{aligned} \Delta N_p=\exp[\alpha(z-z_d)^2]\Bigg\{&\theta_p+\xi_p\,\mathrm{erf}[\alpha^{1/2}(z-z_d)]\\ &+\int_0^z dz'\frac{g(z')}{2D_p}\left(\frac{\pi}{\alpha}\right)^{1/2}\mathrm{erf}[\alpha^{1/2}(z'-z_d)]\\ &-\mathrm{erf}[\alpha^{1/2}(z-z_d)]\int_0^z dz'\frac{g(z')}{2D_p}\left(\frac{\pi}{\alpha}\right)^{1/2}\Bigg\}, \end{aligned} \tag{13}$$

$$\begin{aligned} \Delta N_n=\exp[-\alpha(z-z_d)^2]\Bigg\{&\theta_n+\xi_n F[\alpha^{1/2}(z-z_d)]\\ &+\int_0^z dz'\frac{\alpha^{-1/2}}{D_n}g(z')F[\alpha^{1/2}(z'-z_d)]\\ &-F[\alpha^{1/2}(z-z_d)]\int_0^z dz'\,\alpha^{-1/2}\frac{g(z')}{D_n}\Bigg\} \end{aligned} \tag{14}$$

with $F(x)=\int_0^x \exp(t^2)\,dt$. The constants θ_p, ξ_p, θ_n and ξ_n can be determined using the specific boundary conditions discussed below.

2.3. *Carrier transport in the neutral zone*

The carrier fluxes are reduced to their diffusion components. Moreover, at low injection level ($\Delta N_n \ll N_{n0}$, N_{n0} being the equilibrium density of electrons), the lifetime of a carrier pair is determined by the minority carrier recombination because the deviation from the equilibrium density N_{p0} is more important for these carriers ($\Delta N_p \gg N_{p0}$). Consequently, the excess holes diffuse and recombine at any point of the semiconductor and the electrons follow to maintain local charge neutrality, thus $\Delta N_p = \Delta N_n$ at any point of the neutral region. Hence we need only consider the continuity equation for holes

$$D_p \frac{d^2(\Delta N_p)}{dz^2} = g(z) - \frac{\Delta N_p}{\tau_p}. \tag{15}$$

The general solution of eqn. (15) is

$$\Delta N_p(z) = B_p \exp\left[\frac{-(z-z_d)}{L_p}\right] + \frac{L_p}{2D_p}\int_{z_d}^{\infty} g(z')\left\{\exp\left(\frac{-|z-z'|}{L_p}\right) - \exp\left[\frac{-(z+z'-2z_d)}{L_p}\right]\right\} dz'. \tag{16}$$

The constant B_p is the hole concentration at the limit of the depletion zone, namely $\Delta N_p(z=z_d) = B_p$ and the integral term in eqn. (16) corresponds to the solution given by Wu and Wittry (1978) who used the specific boundary condition $\Delta N_p(z_d) = 0$.

The actual minority carrier flux at the limit $z = z_d$ can be derived from eqn. (16)

$$J_p(z_d) = D_p(B_p/L_p) + J_b^0, \tag{17}$$

where J_b^0 corresponds to the carrier flux at $z = z_d$ calculated by Wu and Wittry. J_b^0 is given in Appendix A.

2.4. *Boundary conditions*

There are five constants which have to be determined: θ_p, ξ_p, θ_n, ξ_n and B_p, and hence five boundary equations have to be written.

Assuming the continuity of the excess carrier concentrations and fluxes at the limit of the depletion zone, we obtain three equations:

$$\Delta N_p(z_d^+) = \Delta N_p(z_d^-), \tag{18}$$

$$\Delta N_p(z_d) = \Delta N_n(z_d) \tag{19}$$

and $J_p(z_d^+) = J_p(z_d^-)$ which implies that

$$\left.\frac{d(\Delta N_p)}{dz}\right|_{z=z_d^+} = \left.\frac{d(\Delta N_p)}{dz}\right|_{z=z_d^-}. \tag{20}$$

At the metal–semiconductor interface, we assume that a fraction J_p^r of the minority carrier flux recombines. The recombination velocity of holes S_p is related to J_p^r by the equation:

$$J_p^r = S_p \Delta N_p(0). \tag{21}$$

At steady state, the occupation ratio of the interface states is kept constant by the recombination of a fraction J_n^r of the majority carriers equal to J_p^r. A recombination velocity S_n can be defined by the relation

$$J_n^r = S_n \Delta N_n(0) \tag{22}$$

with

$$S_n \Delta N_n(0) = S_p \Delta N_p(0). \tag{23}$$

The continuity of the carrier fluxes at the interface leads to the two following equations (see fig. 1):

$$J_p^c = S_p \Delta N_p(0) + J_p(0), \tag{24}$$

$$J_n^c = S_n \Delta N_n(0) + J_n(0), \tag{25}$$

where J_p^c and J_n^c are the collected fluxes of holes and electrons respectively. Similar boundary conditions have been used by Lavagna, Pique and Marfaing (1977) to analyse the quantum photoelectric yield in Schottky diodes. Following these authors, we write the fluxes J_p^c and J_n^c in the form:

$$J_p^c = -V_p \Delta N_p(0), \tag{26}$$

$$J_n^c = -V_n \Delta N_n(0), \tag{27}$$

where V_p and V_n are the collection velocities and can be expressed, assuming a thermionic emission mechanism (Crowell and Sze 1966), as

$$V_{p,n} = A_{p,n}^* T^2/(eN_{v,c}) \tag{28}$$

where $A_{p,n}^*$ are the effective Richardson constants for holes and electrons, N_v and N_c the valence- and conduction-band state densities respectively and T is the temperature.

We report in the table the values obtained using the data given by Sze (1981).

Substituting eqns. (26) and (27) in eqns. (24) and (25) and using eqns. (18), (19) and (20), the constants θ_p, ξ_p, B_p, θ_n and ξ_n can be determined. The expressions obtained are given in the Appendix. Since we have assumed that the majority carrier recombination at the interface is 'induced' by the minority carrier recombination, only the parameter S_p will be considered as a characteristic one, while the recombination velocity of electrons S_n is determined using eqn. (23).

Parameter values for Ge.

D_p ($cm^2 s^{-1}$)	50	These values correspond to the intrinsic mobilities of holes and electrons ($\mu_p = 1900\,cm^2 s^{-1} V^{-1}$, $\mu_n = 3900\,cm^{-2} V^{-1}$) given by Sze (1981).
D_n ($cm^2 s^{-1}$)	97	
V_p ($cm\,s^{-1}$)	$3{\cdot}8 \times 10^6$	
V_n ($cm\,s^{-1}$)	7×10^6	
ε ($F\,cm^{-1}$)	$1{\cdot}4 \times 10^{-12}$	

2.5. *Collection efficiency*

Using eqns. (26) and (27) the total collected current density is

$$|i_c| = eV_p \Delta N_p(0) - eV_n \Delta N_n(0). \tag{29}$$

The collection efficiency η can be expressed as the ratio of collected current to the total charge generation (eqn. (4))

$$\eta = |i_c|/(eG_0). \tag{30}$$

In the following section, we discuss the beam energy dependence of η for Au/n-Ge contacts as predicted by our model and the Wu and Wittry calculations; thus an analysis of some experimental data is considered.

§ 3. Discussion of the model

In addition to the parameters reported in the table and those which characterize the generation function $g(z)$, we have to estimate the pair creation energy ε_{e-h} and the energy loss by the back-scattering process taken into account by the factor f in eqn. (4).

The experimental data for ε_{e-h} usually show a large scatter—from 3·44 to 3·79 eV for GaAs (a list of the experimental values and the corresponding references has been given by Wu and Wittry (1978). Fewer experimental data are available for Ge. Klein (1967) discussed what he called 'the electron–hole pair creation energy puzzle in germanium' and concluded that the 'true' room-temperature mean energy ε_{e-h} is close to 2·80 eV. Such a value has been confirmed by Zulliger (1971) and hence was used for our computations. The factor f can be estimated using the expression proposed by Sternglass (1954) for the mean value E_r of the back-scattered energy:

$$E_r = (0{\cdot}45 + 2 \times 10^{-3} Z) E_0 \tag{31}$$

where E_0 is the beam energy and Z the semiconductor atomic number.

The factor f is given by the relation

$$f = r E_r / E_0, \tag{32}$$

where r is the back-scattering coefficient. The beam energy dependence of r for Ge is small ($r = 0{\cdot}362$ at $E_0 = 5$ keV and 0·334 at $E_0 = 30$ keV (Bishop 1966)). An estimation of r can be made by measuring the ratio $s = (I_0 - I_{abs})/I_0$, where I_0 is the beam current and I_{abs} the absorbed current. Figure 2 gives a typical beam energy dependence of s obtained on our Ge samples. At high beam energy, the secondary electron emission is negligible and the factor s becomes constant and can be equated to the back-scattering coefficient r. For more details see the discussion given by Paz and Borrego (1987). A constant average value close to 0·32 was used for our computations.

The influence of each parameter that has an important physical meaning, such as the diffusion length L_p, the interface recombination velocity S_p, the doping level N_d and the corresponding depletion width z_d, has been analysed.

In fig. 3 (*a*), we show the η–beam-energy curves obtained for different diffusion lengths L_p of holes assuming no recombination at the interface ($S_p = 0$) and no transfer of electrons through the Schottky barrier ($V_n = 0$). The doping level N_d is close to 2×10^{16} cm^{-3} and the depletion width z_d has been assumed close to 0·15 μm.

The most conspicuous feature of these curves as compared to those obtained by the Wu and Wittry calculations (dashed lines) is the discrepancy in the η values, which increases when the diffusion length decreases. To explain this result, it should be remembered that in the Wu and Wittry model the collected EBIC intensity i_c (A cm^{-2}) was calculated as the sum of two terms i_d^0 and i_b^0, which were respectively the contributions of the depletion zone and the neutral region of the semiconductor. i_d^0 was obtained assuming a unit collection probability for the minority carriers which are generated in the DZ, that is

$$i_d^0 = -e \int_{DZ} g(z)\, dz$$

and i_b^0 was expressed as the minority charge flux at the limit of the DZ, namely

$$i_b^0 = -eD_p \left. \frac{d(\Delta N_p)}{dz} \right|_{=z_d}.$$

$\Delta N_p(z)$ was calculated using the specific boundary condition $\Delta N_p(z = z_d) = 0$.

Fig. 2

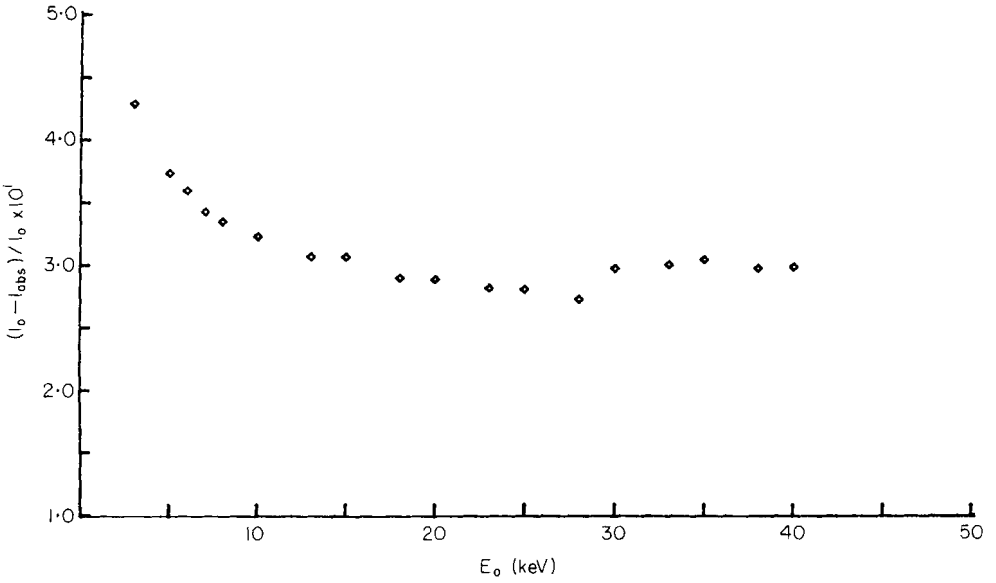

Fraction of the beam intensity lost by the back-scattering and secondary emission processes. I_0 and I_{abs} are the beam intensity and the absorbed intensity respectively. Such measurements are discussed by Paz and Borrego (1987).

It can be easily seen that the actual charge flux at the limit of the DZ i_b as deduced from eqn. (17) is

$$i_b = eD_p(B_p/L_p) + i_b^0. \tag{34}$$

i_b and i_b^0 are both negative quantities due to the z axis orientation (see fig. 1). It is clear from eqn. (34) that the absolute value of i_b is lower than that of i_b^0. Otherwise it has been found that the difference $i_b - i_b^0 = eD_p(B_p/L_p)$ decreases when the diffusion length increases†. From a physical point of view, the boundary condition $\Delta N_p(z_d) = 0$ leads to an overestimation of the excess carrier gradient between the neutral region and the DZ and thus to an 'artificial' increase of the diffusion carrier flux at $z = z_d$. Figures 3 (*b*) and (*c*) compare the η–beam-energy curves obtained for two doping levels ($N_d = 2 \times 10^{14}\,\text{cm}^{-3}$, $z_d = 1{\cdot}5\,\mu\text{m}$) and ($N_d = 2 \times 10^{15}\,\text{cm}^{-3}$, $z_d = 0{\cdot}47\,\mu\text{m}$), assuming transfer of electrons ($V_n = 7 \times 10^6\,\text{cm s}^{-1}$, curve 1) and no transfer ($V_n = 0$, curve 2) of electrons through the Schottky barrier into the metal. It appears clearly that this effect is more significant at low doping levels ($N_d < 10^{15}\,\text{cm}^{-3}$) and for low beam energy. This can be well understood if we note that the electric field intensity near the interface decreases when N_d decreases ($E(z=0) \propto N_d^{1/2}$) and hence becomes insufficiently high at low doping level to reduce notably the electrons excess. Consequently the contribution of electrons ($J_n = V_n \Delta N_n(0)$) cannot be neglected. Figure 3 (*d*) compares the curves

† For $E_0 = 42\,\text{keV}$, $S_p = V_n = 0$, $z_m = 30\,\text{nm}$, $z_d = 1\,\mu\text{m}$ and $N_d = 10^{14}\,\text{cm}^{-3}$, $i_b - i_b^0$ varies by a factor of 20 when L_p varies from 10 to 1 μm.

Fig. 3

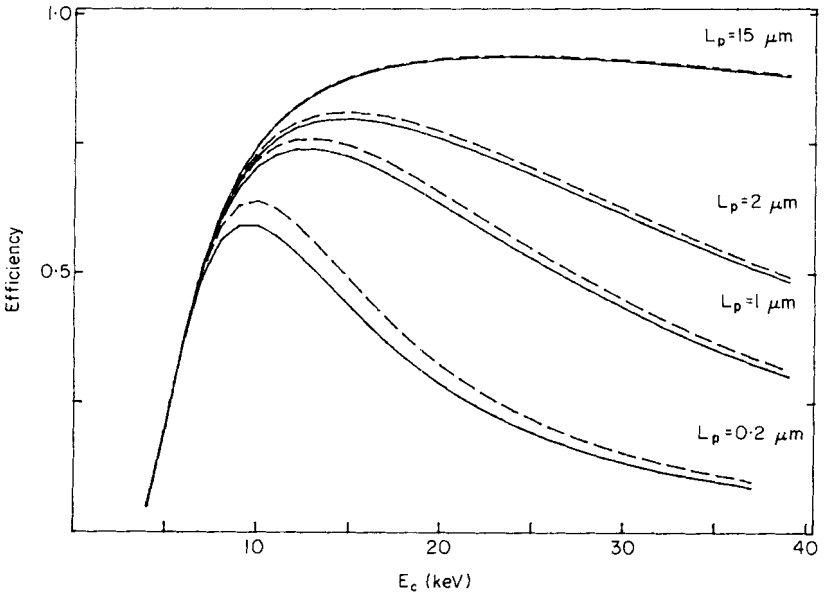
1·0
0·5
Efficiency
L_p=15 μm
L_p=2 μm
L_p=1 μm
L_p=0·2 μm
10
20
30
40
E_c (keV)

(*a*)

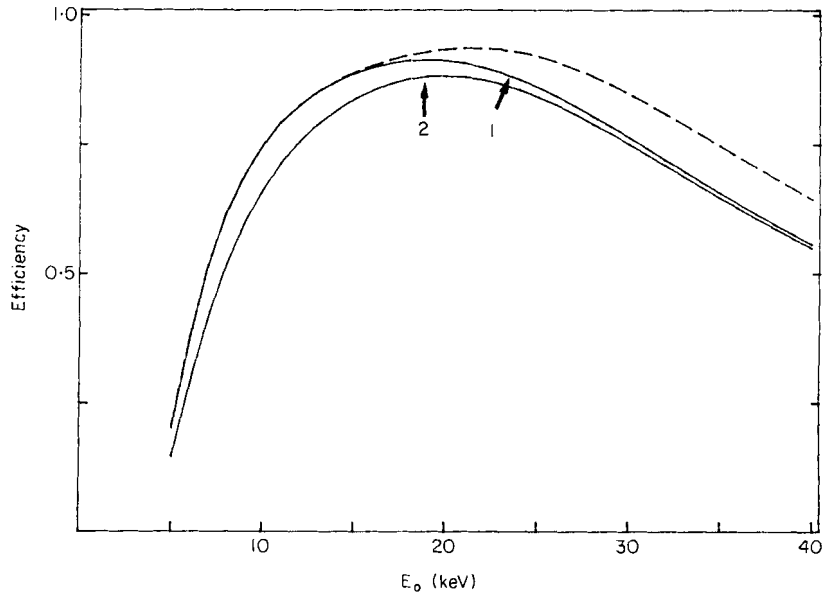
1·0
0·5
Efficiency
2
1
10
20
30
40
E_o (keV)

(*b*)

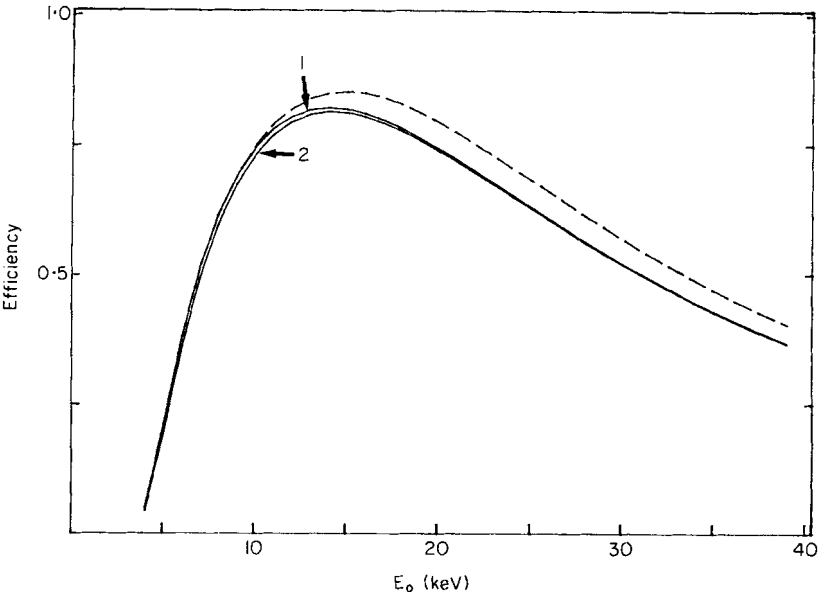
1·0
0·5
Efficiency
1
2
10
20
30
40
E₀ (keV)

(*c*)

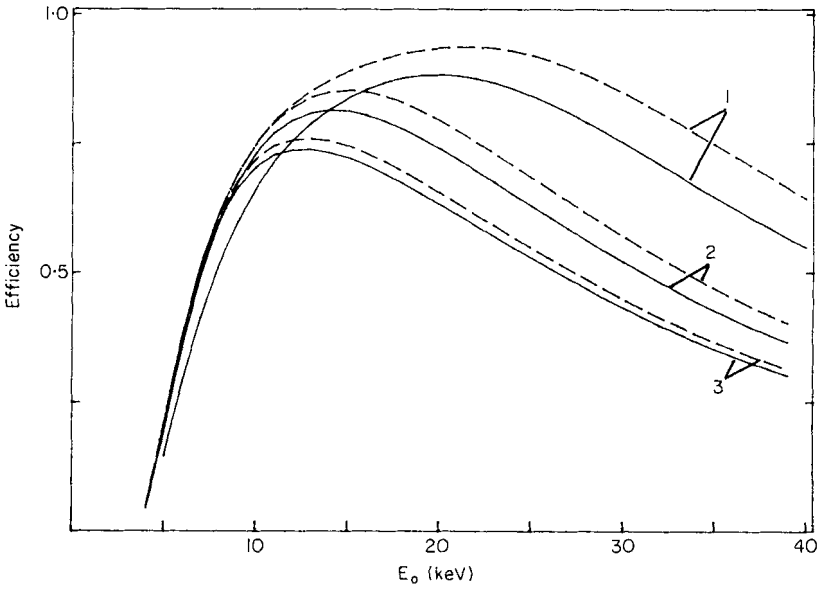
1·0
0·5
Efficiency
1
2
3
10
20
30
40
E₀ (keV)

(*d*)

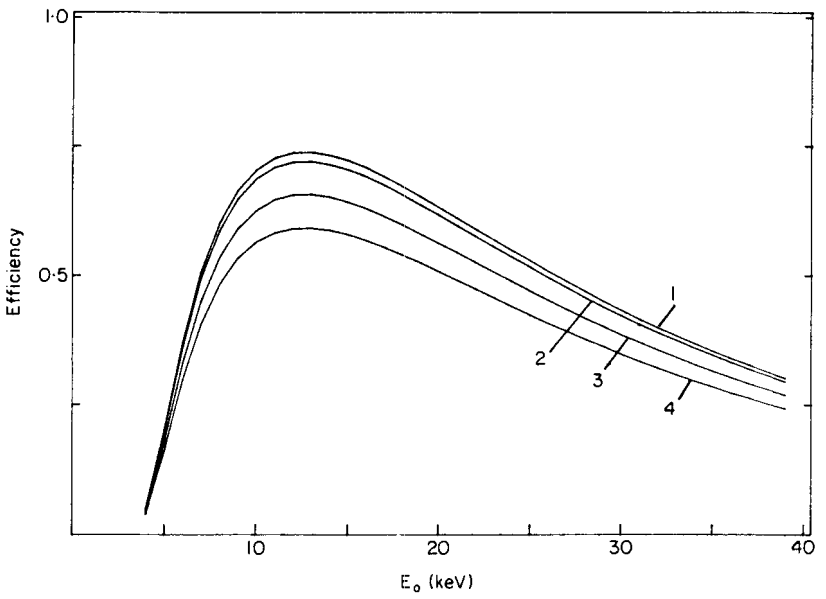

(e)

Curves of η against beam energy at Au–n-Ge Schottky contacts for various parameter values. The solid lines correspond to this model. The dashed lines have been obtained using the Wu and Wittry (1978) model. (*a*) Influence of the hole diffusion length: Metal thickness $z_m = 25$ nm, depletion zone $z_d = 0{\cdot}15$ μm and doping level $N_d = 2 \times 10^{16}$ cm^{-3}. Solid lines are calculated assuming no carrier recombination at the interface ($S_p = 0$). The electron transfer from the semiconductor into the metal has been found negligible. (*b*) Majority carrier injection effect at low doping level: $N_d = 2 \times 10^{14}$ cm^{-3}, $z_m = 25$ nm, $S_p = 0$ and $L_p = 1$ μm. Curve 1 has been obtained for $V_n = 0$ and curve 2 for $V_n = 7 \times 10^6$ cm s^{-1}. Note that the values of curve 2 are lower, particularly at low beam energies, owing to electron transfer into the metal. (*c*) Majority carrier injection effect at moderate doping level: $N_d = 2 \times 10^{15}$ cm^{-3}, $z_d = 0{\cdot}47$ μm, $z_m = 25$ nm, $S_p = 0$ and $L_p = 1$ μm, $V_n = 0$ (curve 1) and $V_n = 7 \times 10^6$ cm s^{-1} (curve 2). Note that the electron transfer into the metal layer is reduced in comparison with the results of fig. 3 (*b*). (*d*) Comparison of the results obtained for various doping levels: $N_d = 2 \times 10^{14}$ cm^{-3}, $z_d = 1{\cdot}5$ μm (curve 1); $N_d = 2 \times 10^{15}$ cm^{-3}, $z_d = 0{\cdot}47$ μm (curve 2); and $N_d = 2 \times 10^{16}$ cm^{-3}, $z_d = 0{\cdot}15$ μm (curve 3). The other parameters were constant at values $z_m = 25$ nm, $S_p = 0$, $V_n = 7 \times 10^6$ cm s^{-1} and $L_p = 1$ μm. (*e*) Influence of the interface recombination velocity S_p: $S_p = 0$ (curve 1), 10^5 cm s^{-1} (curve 2), 5×10^5 cm s^{-1} (curve 3) and 10^6 cm s^{-1} (curve 4). $z_m = 25$ nm, $z_d = 0{\cdot}15$ μm and $L_p = 1$ μm, $N_d = 2 \times 10^{16}$ cm^{-3}.

obtained for three doping levels. It should be pointed out that Wu and Wittry (1978) mentioned that some of their experimental data obtained on lightly doped Si($N_d \simeq 10^{14}$ cm^{-3}) presented a systematic deviation from the theory. The authors invoked the recombination of carriers within the DZ to explain such a deviation, but it seems likely that the majority carrier injection into the metal occurs in this case, which would explain the disagreement between the Wu and Wittry experiments and calculations observed at low beam energy.

We report in fig. 3 (*e*) the η–beam-energy curves obtained for different values of the interface recombination velocity S_p. As expected, the minority carrier loss at the

interface leads to a lowering of the collection efficiency. The effect becomes significant for S_p values higher than $10^5\,\mathrm{cm\,s^{-1}}$.

It appears clearly from the above discussion that the η values are sensitive not only to some physical processes such as the recombination of carriers at the interface and the injection of majority carriers into the metal (for a low doping level and low beam energy), but also to the boundary conditions used. Therefore some caution must be taken in the evaluation of various parameters (z_d, z_m, L_p and ε_{e-h}) using a fitting procedure as is usually done in the literature. It seems more convenient, if it is possible, to determine some of these parameters by other well established techniques such as $C(V)$ and $I(V)$ measurements; then reliable values of the diffusion length L_p and the recombination velocity S_p can be obtained from the fit of the η–beam-energy curves.

§4. Comparison with experiments

Au–Ge evaporated contacts have been obtained on phosphorus-doped bicrystals containing a pure symmetric grain-boundary tilted 3° around [011] with a resistivity of 40 Ω cm and on antimony-doped polycrystals with resistivities of 30 and 0·4 Ω cm. The experimental details have been reported in a previous paper (Tabet and Monty 1988).

The main characteristics of the collection efficiency–beam energy (η–E_0) curves obtained on the three materials are:

(1) Nearly constant η values at high beam energies have been observed. Such results indicate that the minority carrier diffusion length is particularly high in the specimens studied.

(2) Values are lower than those predicted by the Wu and Wittry model and increase more smoothly at low beam energies in our case, particularly in the more resistive samples (40 and 30 Ω cm). In the later cases, the collected EBIC intensity has been corrected by a factor F which takes into account the influence of the resistance R_s of the sample. The short-circuit EBIC intensity I_{cc} can be related to the collected intensity I_c by the following expression (Dianteil 1983):

$$I_{cc}=FI_c, \tag{35}$$

with

$$F=1+\frac{eR_sI_s}{nkT}. \tag{36}$$

I_s is the saturation current of the diode and n the ideality factor. I_s and R_s are deduced from the $I(V)$ characteristic of the Schottky contact. R_s is proportional to the sample thickness and the factor F varies from 1·0 to 1·35. In order to reduce the number of the parameters involved in the fitting procedure of our η–E_0 experimental curves, Hall measurements have been made to determine the doping level N_d. The width of the depletion zone has been estimated using the barrier height deduced from the $I(V)$ characteristics ($\phi_b=0{\cdot}54\,\mathrm{eV}$).

Figures 4(*a*)–(*c*) show the η–E_0 curves obtained on three of the types of samples studied. It can be seen that good fits to the experimental data have been obtained for high recombination velocities ($S_p>5\times10^5\,\mathrm{cm\,s^{-1}}$) at the Au–Ge interface. Moreover, as expected, the diffusion length for the highly doped material ($N_d=10^{16}\,\mathrm{cm^{-3}}$, $L_p=13\,\mu\mathrm{m}$: fig. 4(*a*)) is much lower than the values obtained for the lightly doped

Fig. 4

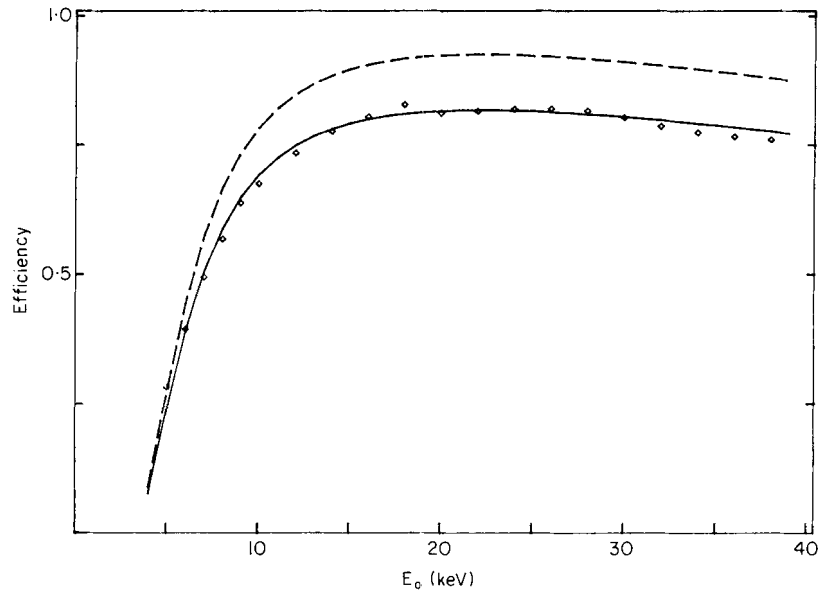
1·0
0·5
Efficiency
10
20
30
40
E₀ (keV)

(*a*)

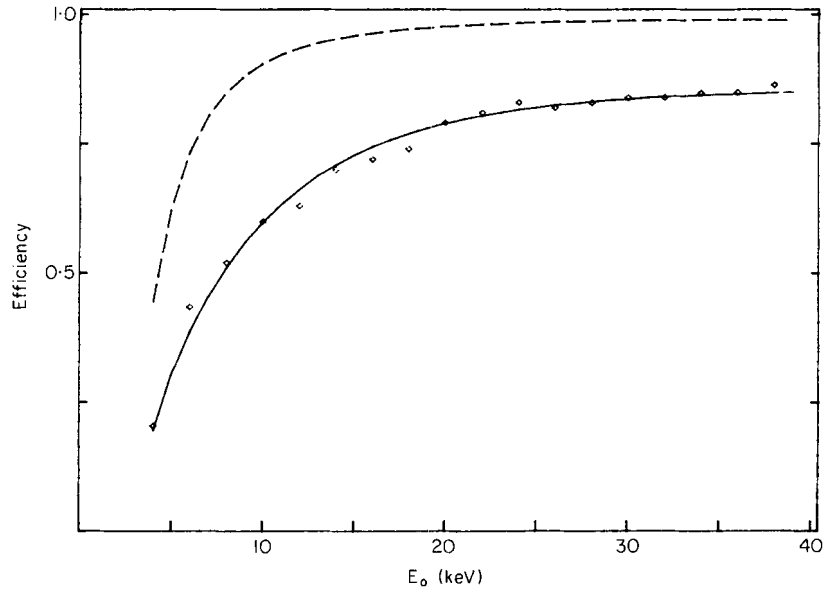
1·0
0·5
Efficiency
10
20
30
40
E₀ (keV)

(*b*)

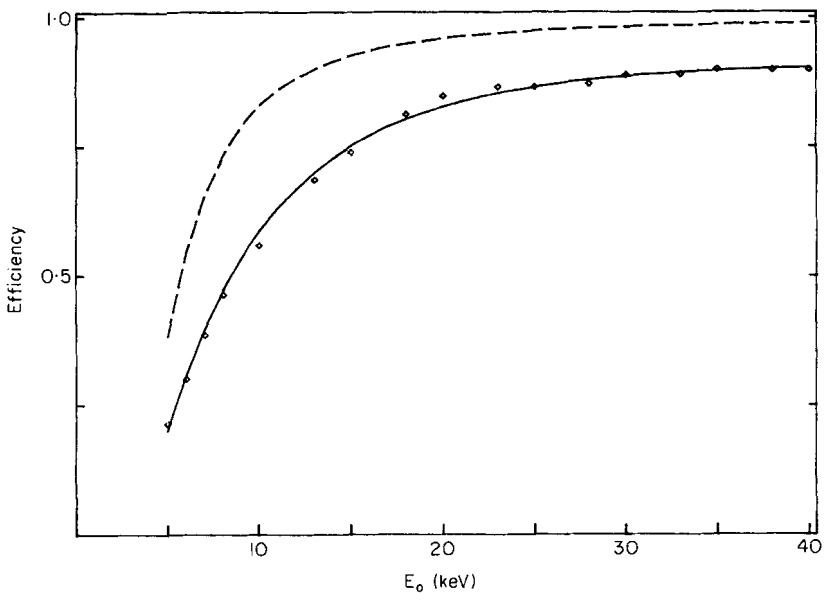

(*c*)

Comparison of theory with the experimental results obtained on various Au–n-Ge Schottky contacts. (◇) are experimental points. Solid lines correspond to theoretical calculations using this model. The dashed lines correspond to the Wu and Wittry model. (*a*) Polycrystalline Sb-doped sample ($N_d = 10^{16}\,cm^{-3}$, $\rho = 0{\cdot}4\,\Omega cm$), $z_m = 22\,nm$, $S_p = 5{\cdot}2 \times 10^5\,cm\,s^{-1}$, $z_d = 0{\cdot}25\,\mu m$, $L_p = 13\,\mu m$. (*b*) Polycrystalline Sb-doped sample ($\rho = 30\,\Omega cm$), $z_d = 2{\cdot}1\,\mu m$, $z_m = 11\,nm$, $S_p = 1{\cdot}2 \times 10^6\,cm\,s^{-1}$, $N_d = 8 \times 10^{13}\,cm^{-3}$, $L_p = 100\,\mu m$. (Any value of $L_p > 100\,\mu m$ gives a similar good fit.) (*c*) Bicrystalline P-doped sample containing pure symmetric grain boundary tilted 3° around [011] ($\rho = 40\,\Omega cm$), $z_m = 18\,nm$, $S_p = 5{\cdot}2 \times 10^5\,cm\,s^{-1}$, $N_d = 8 \times 10^{13}\,cm^{-3}$, $z_d = 2{\cdot}1\,\mu m$, $L_p = 100\,\mu m$. (Any value of $L_p > 100\,\mu m$ gives a similar good fit.)

samples (figs. 4 (*b*) and (*c*)). For the latter, similar good fits can be obtained for any value of L_p higher than 100 μm and consequently reliable values of L_p cannot be deduced from the η–E_0 measurements. However, it is known that this can be done from the EBIC profiles, $I_{EBIC}(x)$, x being the distance from the diode edge. Several authors have proposed various methods to deduce the minority diffusion length from such profiles (Ioannou and Davidson 1979, Davidson and Dimitriadis 1980, Donolato 1984, Kuiken and Van Opdorp 1985). Some of these methods use asymptotic expressions of the EBIC intensity profiles derived from the point-source-generation approximation. The influence of the surface recombination velocity V_s has also been considered by Kuiken and Opdorp (1985). Two extreme cases can be distinguished:

(1) $V_s = 0$: According to the Kuiken and Opdorp calculations, the EBIC intensity can be expressed as:

$$I_{EBIC}(X_s) \propto \operatorname{erfc}(X_s^{1/2}), \tag{37}$$

where $X_s = x/L_p$ is the normalized distance of the point source localized at the surface.

(2) $V_s = \infty$: A simple asymptotic expression has been derived by Ioannou and Davidson (1979)

$$I_{EBIC}(x) \propto x^{-3/2} \exp(-x/L_p). \tag{38}$$

It should be useful to note that for large distances X_s, eqn. (37) can be written in the form

$$I_{EBIC}(x) \propto \left(\frac{L_p}{\pi}\right)^{1/2} x^{-1/2} \exp\left(-\frac{x}{L_p}\right). \tag{39}$$

Considering our results, the EBIC profile tails are well described by such an asymptotic expression as suggested by the linearity of the $\log(x^{1/2} I_{EBIC})$ against x plots shown in fig. 5.

The diffusion length obtained on the highly doped polycrystal varies from 16 to 18 μm (fig. 5 (*a*)). Several η–E_0 curves have been established at various points of the diode made on this sample. The L_p value measured by the fitting procedure varies from 13 to 20 μm, in good agreement with that obtained from the EBIC profiles. High values have been measured on the slightly doped samples: $L_p \simeq 400$ μm from the Sb-doped polycrystal and $L_p = 1{\cdot}82 \times 10^3$ μm for the P-doped bicrystal. The bicrystal was obtained by the Czochralski method using a bicrystalline seed, while the polycrystalline samples were obtained by solidification of a Ge melt in a crucible.

Finally it appears from our results that the η against beam–energy data lead to high recombination velocities at the Au–Ge interface while the EBIC profiles measured on the same samples are well described by asymptotic expressions derived for no recombination of the carriers at the Ge free surface ($V_s = 0$). Moreover, comparable high values of the recombination velocity at the Au–InP interface have been obtained by Peransin, da Silva and Bresse (1986). This leads us to suggest that the Au–Ge interface states that are responsible for the carrier recombination are 'metal-induced states' rather than 'intrinsic Ge surface states'.

Fig. 5

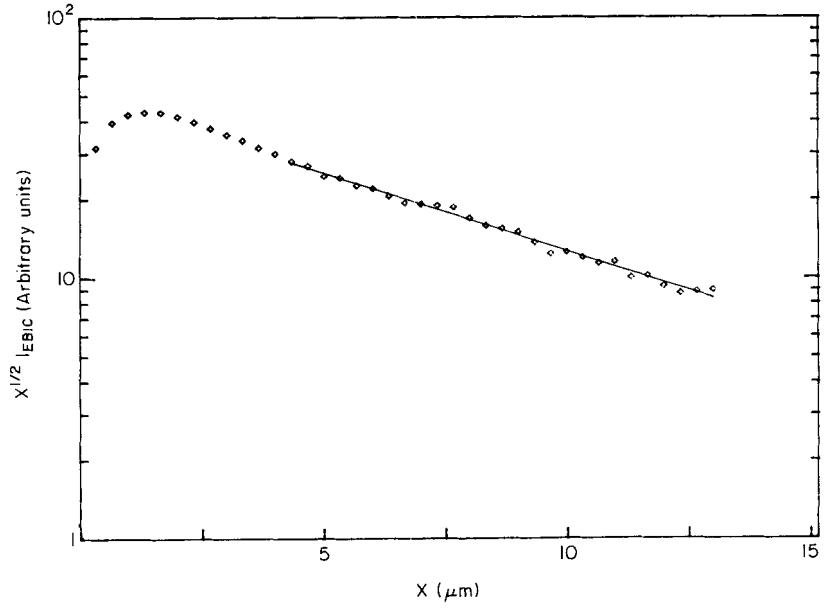

(*a*)

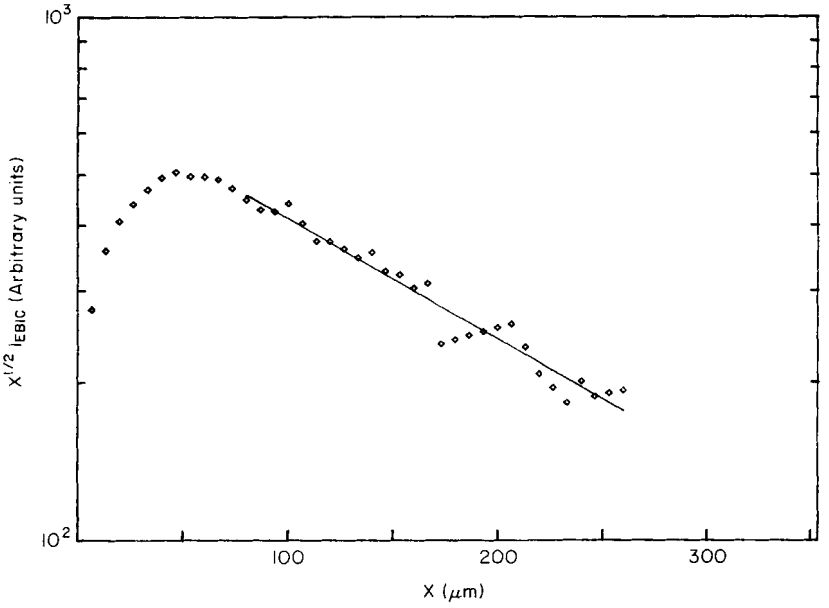

(*b*)

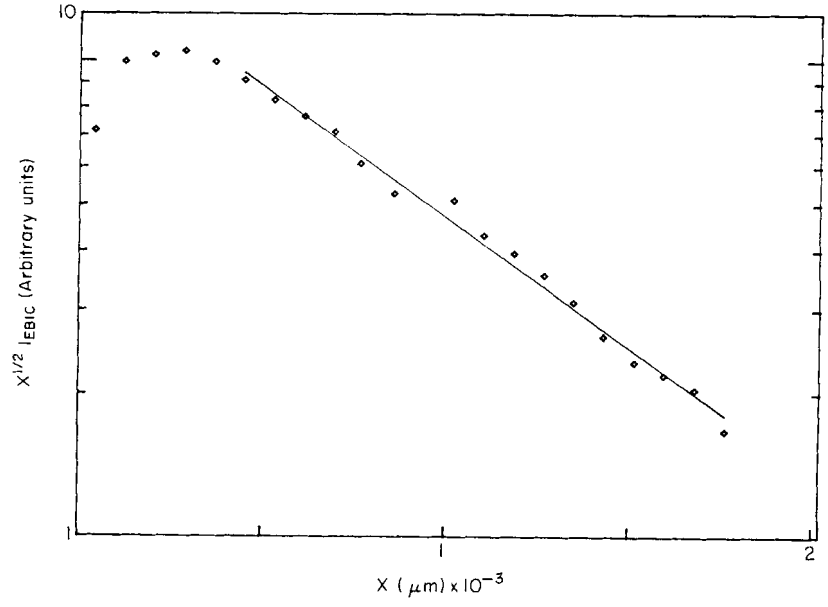

(*c*)

Plots of $\log(x^{1/2}I_{EBIC})$ against x obtained on various Ge samples: (*a*) Sb-doped Ge ($\rho = 0{\cdot}4\,\Omega$ cm), $L_p = 16{\cdot}6\,\mu$m; (*b*) Sb-doped Ge ($\rho = 30\,\Omega$ cm), $L_p = 436\,\mu$m; and (*c*) P-doped Ge ($\rho = 40\,\Omega$ cm), $L_p = 1{\cdot}82 \times 10^3\,\mu$m. The straight lines were obtained by linear regression.

§ 5. Conclusions

A model for EBIC collection has been proposed assuming drift and diffusion of the excess carriers without recombination within the depletion zone of the Schottky contact. The recombination of carriers at the metal–semiconductor interface has been considered and characterized by a recombination velocity S_p. The model allows determination of the minority carrier diffusion length and the recombination velocity S_p which are two important parameters characterizing the device. It has been found that the assumption of a unit collection probability for the minority carriers generated within the depletion zone and the related boundary condition $\Delta N_p(z=z_d)=0$, lead to an overestimation of the collected current particularly for materials with short diffusion lengths. This result must be underlined since the diffusion length is generally obtained from the fit of the experimental curves of η against beam energy.

The majority carrier injection through the Schottky barrier has been found to be non-negligible for a low doping level ($N_d \simeq 10^{14}\,\mathrm{cm}^{-3}$) and low beam energy. The model has been successfully used to analyse the experimental data obtained on Au–n-Ge Schottky contacts.

Finally, it should be pointed out that the EBIC and LBIC contrast observed at defects (grain boundaries and dislocations) are usually modelled using the 100% collection efficiency assumption for the minority carriers within the depletion zone. It does not seem easy to predict how this assumption and the related boundary condition affect the results of the contrast computations. A tentative treatment for EBIC contrast at grain boundaries is in progress.

Acknowledgments

The authors are indebted to Dr Y. Marfaing (L.P.S., Meudon) for helpful discussions and to Drs C. Monty and J. Castaing for their comments on the manuscript. This work was supported by the Agence Française pour la Maîtrise de l'Energie (A.F.M.E.) and Minemet Recherches.

APPENDIX A

Excess carrier flux at $z=z_d$

The minority carrier flux J_b at the limit of the DZ is given by eqn. (17). J_b^0 is the contribution of the integral term in eqn. (16) to the flux and can be expressed in the form given by Wu and Wittry (1978):

$$eJ_b^0 = -eA\left(\frac{\pi^{1/2}\Delta u}{2}\right)\exp\left[aw+\left(\frac{w\Delta u}{2}\right)^2\right]\operatorname{erfc}\left(\frac{a}{\Delta u}+\frac{w\Delta u}{2}\right)+\frac{eB}{(b/u_0)+w}\exp\left(-b\frac{u_s}{u_0}\right),$$

where

$$a=u_m+u_d-u_0, \qquad u_d=\rho z_d/R, \qquad w=R/(\rho L_p), \qquad u_s=u_m+u_d$$

$$\operatorname{erfc}(x)=1-\operatorname{erf}(x), \qquad \operatorname{erf}(x)=\frac{2}{\pi^{1/2}}\int_0^x \exp(-t^2)\,dt.$$

APPENDIX B

Expressions of the integrated constants

For holes, using eqns. (18), (20), (21), (24) and (26), one obtains

$$\xi_p = \frac{G_p - H_p + L_p J_b^0 / D_p}{\operatorname{erf}(-\alpha^{1/2} z_d) - 2L_p(\alpha/\pi)^{1/2} - [2D_p/(S_p + V_p)] \exp(-\alpha z_d^2)(\alpha/\pi)^{1/2}},$$

where

$$G_p = \int_0^{z_d} \left(\frac{\pi}{4\alpha}\right)^{1/2} \operatorname{erf}[\alpha^{1/2}(z' - z_d)] \frac{g(z')}{D_p} dz',$$

$$H_p = \frac{L_p}{D_p} \int_0^{z_d} g(z')\, dz',$$

$$\theta_p = -\xi_p \frac{D_p}{V_p + S_p} \exp(-\alpha z_d^2) \left[\frac{V_p + S_p}{D_p} \operatorname{erf}(-\alpha^{1/2} z_d) \exp(\alpha z_d^2) - 2\left(\frac{\alpha}{\pi}\right)^{1/2}\right]$$

$$= H_p - G_p - \frac{L_p}{D_p} J_b^0 - 2L_p \left(\frac{\alpha}{\pi}\right)^{1/2} \xi_p,$$

$$B_p = \theta_p + G_p = H_p - \frac{L_p}{D_p} J_b^0 - 2L_p \left(\frac{\alpha}{\pi}\right)^{1/2} \xi_p.$$

For electrons, using eqns. (19), (23), (25) and (27), one obtains

$$\theta_n = B_p + G_n,$$

where

$$G_n = \int_0^{z_d} \alpha^{-1/2} \frac{g(z')}{D_n} F[\alpha^{1/2}(z' - z_d)]\, dz',$$

$$F(x) = \int_0^x \exp(t^2)\, dt$$

$$\xi_n = \left[\frac{S_p \Delta N_{p0}}{D_n} + \theta_n \frac{V_n}{D_n} \exp(-\alpha z_d^2)\right] \Big/ \left[\alpha^{1/2} - \frac{V_n}{D_n} \exp(\alpha z_d^2) F(-\alpha^{1/2} z_d)\right],$$

where ΔN_{p_0} is given by

$$\Delta N_{p_0} = [\theta_p + \xi_p \operatorname{erf}(-\alpha^{1/2} z_d)] \exp(\alpha z_d^2).$$

REFERENCES

BISHOP, H. E., 1966; cited in THORNTON, P. R., 1968, *Scanning Electron Microscopy. Applications to Materials and Device Science* (London: Chapman and Hall).

CROWELL, C. R., and SZE, S. M., 1966, *Solid St. Electron.*, **9**, 1035.

DAVIDSON, S. M., and DIMITRIADIS, C. A., 1980, *J. Microsc.*, **118**, 275.

DIANTEIL, C., 1983, Thèse Docteur Ingénieur, Université Paul Sabatier de Toulouse.

DONOLATO, C., 1984, *IEEE Trans. Electron Devices*, **31**, 121.

HOLT, D. B., MUIR, M. D., GRANT, P. R., and BOSWARVA, I. M., 1974, *Quantitative Scanning Electron Microscopy* (London: Academic Press).

KLEIN, C. A., 1967, *Phys. Lett.* A, **24**, 513.

KUIKEN, H. K., and VAN OPDORP, C., 1985, *J. appl. Phys.*, **57**, 2077.

IOANNOU, D. E., and DAVIDSON, S. M., 1979, *J. Phys.* D, **12**, 1339.

LAVAGNA, M., PIQUE, J. P., and MARFAING, Y., 1977, *Solid St. Electron.*, **20**, 235.

LEAMY, H. J., 1982, *J. appl. Phys.*, **53,** 1454.
PAZ, O., and BORREGO, J. M., 1987, *J. appl. Phys.*, **61,** 1537.
PERANSIN, J. M., DA SILVA, B. E. F., and BRESSE, J. F., 1986, *Phys. Stat. sol.* (a), **94,** 713.
RHODERICK, E. H., 1978, *Metal–Semiconductor Contacts* (Oxford: Clarendon Press).
SIEBER, B., 1987, *Phil. Mag.* B, **55,** 5, 585.
STERNGLASS, E. J., 1954, *Phys. Rev.*, **95,** 345.
SZE, S. M., 1981, *Physics of Semiconductor Devices.* Second Edition (New York: John Wiley), p. 850.
TABET, N., and MONTY, C., 1988, *Phil. Mag.* B, **57,** 763.
TERSOFF, J., 1984, *Phys. Rev.*, **30,** 4874.
WITTRY, D. B., and KYSER, D. F., 1967, *J. appl. Phys.*, **38,** 375.
WU, C. J., and WITTRY, D. B., 1978, *J. appl. Phys.*, **49,** 2827.
ZULLIGER, H. R., 1971, *J. appl. Phys.*, **42,** 5570.